

UCSF

UC San Francisco Previously Published Works

Title

Impairment of NK cell function by NKG2D modulation in NOD mice

Permalink

<https://escholarship.org/uc/item/8tp238w5>

Journal

Immunity, 18(1)

ISSN

1074-7613

Authors

Ogasawara, Kouetsu
Hamerman, Jessica A
Hsin, Honor
et al.

Publication Date

2003

Peer reviewed

Impairment of NK cell function by NKG2D modulation in NOD mice

Kouetsu Ogasawara¹, Jessica A. Hamerman¹, Honor Hsin², Shunsuke Chikuma²,
Helene Bour-Jordan², Taian Chen¹, Thomas Pertel¹, Claude Carnaud³,
Jeffrey A. Bluestone^{2,4}, and Lewis L. Lanier^{1,4}

¹Department of Microbiology & Immunology and the Cancer Research Institute,

University of California, San Francisco

513 Parnassus Ave. HSE 420, Box 0414, San Francisco, California 94143-0414, USA

²Diabetes Center, University of California, San Francisco

513 Parnassus Ave. HSW 1114, Box 0540, San Francisco, California 94143-0540, USA

³INSERM U25 – Hopital Necker, 161, Rue de Sevres, 75743 Paris Cedex 15, France

Correspondence should be addressed to: L.L.L. (lanier@itsa.ucsf.edu)

Phone: 415-514-0829 FAX: 509-275-1244

⁴Co-senior authors

Running title: NKG2D in NOD mice

Summary

Non-obese diabetic (NOD) mice, a model of insulin-dependent diabetes mellitus, have a defect in natural killer (NK) cell-mediated functions. Here we show impairment in an activating receptor, NKG2D, in NOD NK cells. While resting NK cells from C57BL/6 and NOD mice expressed equivalent levels of NKG2D, upon activation NOD NK cells, but not C57BL/6 NK cells, expressed NKG2D ligands, which resulted in down-modulation of the receptor. NKG2D-dependent cytotoxicity and cytokine production were decreased because of receptor modulation, accounting for the dysfunction. Modulation of NKG2D was mostly dependent on the YxxM motif of DAP10, the NKG2D-associated adapter that activates phosphoinositide 3 kinase. These results suggest that NK cells may be desensitized by exposure to NKG2D ligands.

Introduction

Insulin-dependent diabetes mellitus (IDDM) is a multi-factorial autoimmune disease characterized by the destruction of insulin-producing β cells by auto-reactive T lymphocytes in the pancreas (Bach, 1994; Castano and Eisenbarth, 1990). Accompanying T cell dependent autoimmune responses, IDDM patients and non-obese diabetic (NOD) mice demonstrate impaired immune responses against certain pathogens (Attallah et al., 1987; Cameron et al., 1998; Kataoka et al., 1983). In addition, several reports suggest that natural killer (NK) cell-mediated functions may be abnormal in IDDM patients and NOD mice (Carnaud et al., 2001; Kataoka et al., 1983; Nair et al., 1986; Negishi et al., 1986; Poulton et al., 2001). Indeed, cytotoxicity of NK cells from NOD mice and certain IDDM patients against NK-sensitive tumor cell targets (e.g. K562 and YAC-1) is lower than that observed when using NK cells from normal, healthy mice or humans (Carnaud et al., 2001; Kataoka et al., 1983; Nair et al., 1986; Negishi et al., 1986; Poulton et al., 2001). However, the molecular mechanisms underlying the NK cell abnormalities in IDDM patients and NOD mice are not defined.

NK cells play important roles in immune defense against viral, bacterial and parasitic infections by killing infected cells directly and producing inflammatory cytokines, such as interferon (IFN) $-\gamma$ and tumor necrosis factor (TNF) $-\alpha$ (Biron et al., 1999; Trinchieri, 1989). To accomplish these functions, NK cells recognize target cells through a diverse array of activating receptors (Lanier, 1998). One of the activating receptors, NKG2D (Bauer et al., 1999), is a co-stimulatory receptor expressed on NK cells, NKT cells, $CD8^+$ T cells, $\gamma\delta$ T cells and activated macrophages. NKG2D is associated with a transmembrane adapter molecule, DAP10, which has a YxxM motif that recruits the p85 phosphoinositide-3 (PI3) kinase subunit (Wu et al., 1999). Therefore, NKG2D-dependent activation utilizes the PI3 kinase pathway. Recent studies revealed that cytotoxicity of

mouse NK cells against YAC-1 mainly depends on NKG2D (Jamieson et al., 2002).

Genomic linkage analysis in NOD mice has revealed several *insulin-dependent diabetes (Idd)* loci (Wicker et al., 1995). Interestingly, gene(s) conferring susceptibility to diabetes in NOD mice (Ghosh et al., 1993) have been mapped to a region on chromosome 6 designated the *natural-killer-gene complex (NKC)* that contains a cluster of genes preferentially expressed by NK cells (Rogner et al., 2001; Yokoyama and Seaman, 1993), including NKG2D (*NKG2D* is within the *NKC* (Ho et al., 1998)). Thus, we examined NKG2D-dependent cytotoxicity and IFN- γ production in NOD mice and investigated whether the underlying NK cell abnormalities of NOD mice may involve the NKG2D-dependent activation pathway.

Results

Impaired NKG2D-dependent cytotoxicity and IFN- γ production in activated NOD NK cells

In this study, we compared NKG2D-dependent immune responses using IL-2 activated NK cells from NOD and NK1.1 congenic NOD (NK1.1 NOD) mice. Because *Nkrp1* (NK1.1) is linked closely with *NKG2D*, the *NKG2D* gene in the NK1.1 congenic NOD mice is expected to be derived from the C57BL/6 strain (Carnaud et al., 2001). NK cell-mediated cytotoxicity against YAC-1 target cells is primarily dependent upon NKG2D-dependent activation (Jamieson et al., 2002 and our publications). Consistent with prior reports, cytotoxic activity of NOD NK cells against YAC-1 was significantly less than C57BL/6 NK cells (Fig. 1a). Activated NK cells from NK1.1-congenic NOD mice also demonstrated less cytotoxicity against YAC-1 targets compared with the lytic activity of C57BL/6 NK cells. In addition, anti-NKG2D monoclonal antibody (a-NKG2D mAb) efficiently inhibited cytotoxicity against YAC-1 by NK cells from all strains of mice (Fig. 1a). To directly evaluate the function of NKG2D-mediated cytotoxicity, we analyzed the ability of activated C57BL/6 and NOD NK cells to kill Ba/F3 pro-B cells transfected with a NKG2D ligand, RAE-1 γ (Cerwenka et al., 2000). Only low levels of cytotoxicity were observed against BaF/3 mock transfectants using NK cells from all strains of mice. In contrast, the NKG2D-dependent cytotoxicity against RAE-1 transfectants was remarkably less using activated NK cells from NOD or NK1.1 NOD mice compared with C57BL/6 NK cells (Fig. 1b). NKG2D-dependent cytotoxicity of these NK cells was completely abrogated by a-NKG2D mAb (Fig. 1b). Thus, these findings suggest that a defect in the NKG2D-dependent activation pathway in NOD and NK1.1 NOD NK cells may be responsible for the diminished cytotoxicity against YAC-1 target cells. In addition, we found that NKG2D-dependent IFN- γ production, induced by cross linking with anti-NKG2D mAb,

was reduced using activated NK cells from NOD or NK1.1 NOD mice as compared with that produced by activated C57BL/6 NK cells (Fig. 1c). These results indicated that NKG2D-dependent functions are decreased in activated NK1.1 NOD and NOD NK cells.

NKG2D expression on NOD NK cells

To explain the abnormal NKG2D function in NOD NK cells, we examined NKG2D expression on NK1.1 NOD, NOD and C57BL/6 NK cells. While low but comparable levels of NKG2D were observed on fresh NK cells from these strains (data not shown), NKG2D expression was dramatically decreased in activated NK cells from NOD and NK1.1 NOD mice as compared to C57BL/6 NK cells (Fig. 2a). The decrease in NKG2D expression on NOD NK cells was selective since the expression levels of CD44 and NK1.1 expression were equivalent to C57BL/6 NK cells (Fig. 2a). To determine whether the decrease in NKG2D surface expression was caused by transcriptional regulation, we measured mRNA expression of NKG2D and DAP10 in NK cells by real-time quantitative PCR. Prior studies have shown that expression of NKG2D on the cell surface requires its association with DAP10 (Wu et al., 1999). As shown in Fig. 2b, NOD NK cells expressed equivalent of NKG2D and DAP10 mRNA compared to C57BL/6 NK cells, excluding differential transcription as the cause for diminished NKG2D expression on NOD NK cells.

An alternative possibility to account for the difference between NKG2D expression on NOD versus C57BL/6 NK cells was ligand-induced modulation of NKG2D in NOD NK cells. Unexpectedly, we found that activated NK cells from NOD and NK1.1 NOD mice expressed ligands for NKG2D whereas NKG2D ligands were undetectable on NK cells from C57BL/6 mice (Fig.2c). Moreover, the presence of RAE-1 in activated NOD NK cells, but not C57BL/6 NK cells, was confirmed by analyzing RAE-1 mRNA expression using real-time quantitative RT-PCR (Fig. 2d). Transcripts of RAE-1 α , β , and γ and H-60

were detected in NOD activated NK cells. By contrast, transcripts for NKG2D ligands were not present in NK cells from C57BL/6 mice (Fig. 2d). In addition, activated NK cells from NOD and NK1.1 NOD mice stained positively with a mouse NKG2D-Ig fusion protein and this was confirmed using an anti-RAE-1 specific mAb (Fig. 2e). These results suggest that ligand-dependent modulation of NKG2D may account for the impairment in NKG2D-dependent function in NOD NK cells.

Ligand-induced NKG2D modulation

We investigated whether NKG2D is modulated by the interaction with its ligands. C57BL/6 NK cells were co-cultured with B16 melanoma cells transfected with RAE-1 ϵ or mock transfectants. Although no difference was observed in CD44 expression, NKG2D expression on NK cells was dramatically decreased after co-culture with RAE-1 ϵ bearing transfectants as compared to NK cells co-cultured with mock transfectants (Fig. 3a) or NK cells cultured in the absence of target cells (data not shown). NK cells were harvested and assayed for cytolytic activity against YAC-1 targets. The diminished levels of NKG2D on NK cells co-cultured with RAE-1 transfectants correlated with the impaired cytolytic activity against YAC-1 (killing was ~40% less than that with NK cells co-cultured with mock transfectants) (Fig. 3b). Similar results were obtained using RAE-1 transfected cells as targets in cytotoxicity assays (Fig. 3c). In addition, NKG2D-dependent IFN- γ production was decreased substantially in NK cells previously co-cultured with RAE-1 transfectants as compared with NK cells co-cultured with mock transfectants (Fig. 3d).

To examine whether NKG2D is also modulated on NK cells *in vivo*, we injected RAE-1 γ transfected RMA cells or mock-transfected RMA cells into the spleen of C57BL/6 mice. After 5 days, splenocytes were harvested and analyzed by flow cytometry. Although no difference was observed in NK1.1 (data not shown) or CD44 expression on NK cells

from mice injected with RAE-1 γ^+ RMA cells or mock RMA cells, the levels of NKG2D were substantially reduced on NK cells from mice injected with RAE-1 γ^+ RMA transfectants (Fig. 3e). Furthermore, we investigated whether NKG2D modulation was reversible. NK cells were co-cultured with irradiated RAE-1 ϵ^+ B16 or mock-transfected B16 cells and ligand-induced modulation of NKG2D was confirmed. NK cells were harvested and purified to remove residual tumor cells and then cultured in IL-2 only for 24 hr. In the absence of ligand, expression of NKG2D was restored to normal levels (Fig. 3f). Therefore, NKG2D modulation was reversible. These results indicate that NKG2D modulation is caused by the interaction with NKG2D ligands, which in turn leads to a decrease in NKG2D-dependent cytotoxicity and IFN- γ production.

DAP10-mediated PI3 kinase activation augments ligand-induced NKG2D modulation

To further elucidate the mechanism of NKG2D modulation, we established an *in vitro* model using transfectants of Ba/F3 expressing mouse NKG2D and DAP10. Ba/F3 is a transformed pro-B cell line lacking NK cell function. This permits analysis of interactions of NKG2D with ligand in the absence of target cell killing or other potential pathways involved in NK cell activation. NKG2D+DAP10-Ba/F3 cells were co-cultured with RAE-1 γ transfected RMA (RMA -RAE-1 γ) cells or mock-transfected RMA cells. After 24 hrs, NKG2D expression on the Ba/F3 transfectants was modulated by co-culture with RAE-1 γ -transfected RMA cells, but not mock-transfected RMA cells (Fig. 4a). To exclude the possibility that NKG2D was masked by the presence of RAE-1 protein that was shed from the RAE-1 transfectants, rather than due to ligand-induced receptor modulation, the NKG2D+DAP10-Ba/F3 cells co-cultured with RAE-1 γ^+ RMA were washed briefly in acidic buffer (pH 4.0) before staining with anti-NKG2D mAb. While washing with acidic buffer completely removed soluble NKG2D ligand (i.e. an H-60-Ig fusion protein

(Cerwenka et al., 2000)) from NKG2D+DAP10-Ba/F3 transfectants (data not shown), this treatment did not reveal expression of NKG2D on the cells co-cultured overnight with RAE-1 γ^+ RMA cells (Fig. 4a). Furthermore, the DAP10 protein expressed in the NKG2D transfectants had an N-terminal Flag epitope tag that also demonstrated down-regulation after ligand-induced modulation of NKG2D (data not shown). Together, these results indicated that the observed decreased levels of NKG2D were due to receptor modulation, rather than masking by soluble ligand.

To determine whether NKG2D was internalized after binding RAE-1, the NKG2D bearing cells after co-culture with RAE-1 transfectants were fixed, permeabilized and analyzed for the presence of intracytoplasmic NKG2D. While the amount of NKG2D on the cell surface was reduced on cells co-cultured with RAE-1 transfectants, no difference was observed in the total amount of NKG2D detected by staining of permeabilized cells, which permits detection of both surface and cytoplasmic antigen (Fig. 4b). Therefore, modulation of NKG2D may be caused by internalization. To determine whether degradation in lysosomes is involved in NKG2D down modulation, we treated NKG2D-DAP10 transfectants co-cultured with RAE-1 transfectants with the lysosome inhibitors, NH_4Cl , or chloroquine. In the Ba/F3 transfectants, NKG2D modulation was not influenced by the lysosome inhibitors (Fig. 4c), suggesting that NKG2D down-modulation was independent of the lysosomal compartment. Endocytosis can be mediated by either clathrin-dependent or clathrin-independent mechanisms. Because clathrin-dependent endocytosis is inhibited by hypertonic conditions (Cefai et al., 1998; Rapoport et al., 1997; Sorkin and Carpenter, 1993), we investigated whether this would affect NKG2D modulation. As shown Fig. 4d, NKG2D modulation was inhibited in hypertonic medium (0.45 M sucrose), suggesting that clathrin-dependent endocytosis may be involved in NKG2D modulation.

Further studies were conducted to determine whether signaling is required for efficient ligand-induced modulation of NKG2D. DAP10 possesses a YxxM motif, which binds to the p85 subunit of PI3 kinase and Grb-2 (Chang et al., 1999; Wu et al., 1999). In addition, it is possible that the clathrin adapter complex AP-1 and/or AP-2 will bind the YxxM motif (Brodsky et al., 2001). We examined whether the YxxM motif of DAP10 binds to AP-2 clathrin adaptor complexes. However, we could not detect AP-2 association with DAP10 (data not shown). These findings prompted us to examine whether PI3 kinase activity is involved in NKG2D modulation. To this end, NKG2D - DAP10 Ba/F3 transfectants were co-cultured with RAE-1 transfectants in the presence of the PI3 kinase inhibitor, LY294002. In the presence of the PI3 kinase inhibitor, substantially less modulation of NKG2D was observed, compared to the amount of ligand-induced receptor modulation that was induced in the absence of the drug (Fig. 4e). To further confirm the participation of DAP10 in receptor modulation, we generated Ba/F3 transfectants expressing NKG2D and a DAP 10 protein with a Y-F mutation in the YxxM motif (DAP10 Y-F mut-Ba/F3). The NKG2D - mutant DAP10 complex was expressed at a similar level as wild-type NKG2D - DAP10 in the Ba/F3 transfectants. Ligand-induced modulation of NKG2D was remarkably less efficient in transfectants expressing the mutant DAP10 compared with wild-type DAP10 (Fig.4f), suggesting that DAP10-mediated signal transduction is involved. However, partial NKG2D modulation was observed in the DAP10 mutant transfectant, similar to results obtained using the PI3 kinase inhibitor.

Discussion

In this study, we established that the impaired functions of NK cells in NOD mice are at least in part caused by NKG2D modulation on activated NK cells. Diminished NKG2D on activated NOD NK cells was secondary to ligand-induced internalization of the receptor. Further studies determined that activation of PI3 kinase through the YxxM motif of DAP10 is involved in this process. In this regard, modulation of NKG2D on NK cells and CD28 on T cells is similar (Cefai et al., 1998), but distinct from CTLA-4 modulation (Schneider et al., 1999). While expression of CTLA-4 is regulated by AP-2 binding, we could not detect AP-2 binding to phosphorylated or non-phosphorylated DAP10, similar to what was reported previously for CD28 (Schneider et al., 1999). However, modulation of NKG2D was inhibited in hypertonic medium, suggesting that endocytosis of NKG2D may utilize a clathrin coated-pit dependent pathway, similar to CD28 (Schneider et al., 1999) and epidermal growth factor receptor (Sorkin and Carpenter, 1993).

A striking difference between NK cells from C57BL/6 and NOD mice was the finding that NK cell activation induced the RAE-1 ligands of NKG2D in NOD, but not C57BL/6 NK cells. Thus, in NOD mice both the NKG2D receptor and its ligands are expressed on the same NK cell, which may cause self-modulation of NKG2D expression and function. The difference between NK cells in NOD and C57BL/6 appears to be determined at the level of expression of RAE-1 and not the NKG2D receptor. Indeed, the nucleotide sequences of coding regions of NKG2D and DAP10 are identical in NOD and C57BL/6 mice (unpublished observation) and we show that these genes were transcribed in equal amounts in NOD and C57BL/6 NK cells. Furthermore, activated NK cells from NK1.1 congenic NOD mice, which have both the NK1.1 allele and the linked *NKG2D* locus from C57BL/6, demonstrated diminished NKG2D expression and function. It should be noted that the *RAE-1* genes are not linked to NK1.1; therefore, the *RAE-1* genes are of

NOD origin in the NK1.1 NOD congenic mice. When C57BL/6 NK cells were co-cultured with transfectants expressing RAE-1, NKG2D on the NK cells was modulated and NKG2D-dependent functions were impaired to an extent comparable to activated NOD NK cells. This phenotype was reversible, since NKG2D expression and function recovered when C57BL/6 NK cells were further cultured in the absence of ligand-bearing cells. Consistent with our study, previous reports have demonstrated that NK cell cytotoxicity was decreased following exposure to target cells and the cytolytic activity was recovered following culture in the presence of activating cytokines (Abrams and Brahmi, 1988; Jewett and Bonavida, 1995; Perussia and Trinchieri, 1981; Timonen et al., 1979) It is noteworthy that the NKG2D ligands are remarkably different in C57BL/6 and NOD mice. NOD mice express RAE-1 α , β , and γ and H-60, whereas C57BL/6 mice lack these ligands but instead express RAE-1 δ and ϵ (Cerwenka and Lanier, 2001). As yet, little is known about the transcriptional regulation of *RAE-1* gene expression, but our findings suggest that the *RAE-1* genes in NOD are induced in NK cells by activation, whereas in C57BL/6 they are not. Similarly, the ligands of NKG2D in humans (i.e. MICA, MICB, and ULBP) are polymorphic, whereas DAP10 and NKG2D in mice and human are monomorphic. It will be of interest to determine whether NKG2D expression and function in human NK cells is influenced by the induction of NKG2D ligands on NK cells in certain individuals.

NKG2D-dependent cytotoxicity was also reduced in fresh NOD NK cells as compared with C57BL/6 NK cells (data not shown). However, the expression levels of NKG2D in fresh NOD and NK1.1NOD NK cells were similar to fresh C57BL/6 NK cells (data not shown). As reported previously, the NK cell abnormalities in NOD mice and IDDM patients may be due to multiple defects (Attallah et al., 1987; Poulton et al., 2001; Shultz et al., 1995). Therefore, NK cell defects other than NKG2D modulation may be present in NOD mice.

We found that the interaction of RAE-1 and NKG2D on NK cells induced dysfunction of activated NK cells. In the case of NOD NK cells, this could be caused by modulation of NKG2D by ligand expression within the cytoplasm of the NK cells themselves, because NOD NK cells express both receptor and ligands. Interactions between C57BL/6 NK cells, which do not express NKG2D ligands, and tumors expressing RAE-1 resulted in modulation of receptor expression and function. This was demonstrated *in vitro*, but also was observed on NK cells isolated from the spleen (but not the liver) of mice that received an intrasplenic injection of a lymphoma transfected with RAE-1. These data indicated that NKG2D on NK cells was modulated by the interaction with RAE-1 *in vivo* in the local microenvironment. Initial interactions between NK cells and NKG2D ligand-bearing cells may trigger killing and cytokine production. However, prolonged exposure to ligands may de-sensitize NK cells rendering them functionally anergic. This has implications in the context of tumor development because secretion of soluble NKG2D ligands by tumors (*Groh et al., 2002*) or prolonged exposure of NK cells to ligand-bearing tumors may render them dysfunctional. This may contribute to tumor escape from NK cell and CD8⁺ T cell immune surveillance.

NKG2D may also play a role in autoimmunity. If NKG2D ligands are induced due to inflammation or perhaps inappropriately over-expressed in autoimmune-predisposed individuals, this may exacerbate the disease. In the case of IDDM, perhaps over-expression of NKG2D ligands in the pancreas of certain predisposed individuals may co-stimulate autoreactive CD8⁺ T cells, thereby inducing or augmenting the disease. In preliminary studies, we have detected transcription of *RAE-1* genes in the pancreas of diseased NOD mice, but not young, healthy mice. Of particular interest is the remarkable polymorphism of the genes encoding the NKG2D ligands in mice and human (e.g. more than 50 alleles of human MICA have been identified). Polymorphisms of human MICA have been

associated with a variety of autoimmune disorders, including type I diabetes, ulcerative colitis, primary sclerosing cholangitis, familial Mediterranean fever, and Behcet's disease (Mizuki et al., 1997; Norris et al., 2001; Sugimura et al., 2001; Touitou et al., 2001; Wallace et al., 1999). Whether expression of NKG2D ligands is involved in the induction of disease or only results as a consequence of inflammation is unknown. Nonetheless, our findings suggest that the NKG2D pathway should be considered in autoimmune disease, as well as cancer.

Experimental Procedures

Mice

Six to eight week-old C57BL/6 mice were purchased from Charles River, (Wilmington, MA). NOD mice were obtained from Taconic (Germantown, NY). NK1.1-congenic NOD mice were generated as described previously (Carnaud et al., 2001). Experiments were performed using gender and age-matched mice. All mice were maintained under specific pathogen-free conditions in the animal facility of the University of California, San Francisco (UCSF). All experiments were performed according to the guidelines of the UCSF Committee on Animal Research.

Reagents, cytokines and antibodies

Human recombinant Interleukin (IL)-2 was generously provided by the NCI BRB Preclinical Repository. Mouse recombinant IL-12 was kindly provided by Dr. J.P. Houchins (R&D Systems, Minneapolis, MN). The PI3 kinase inhibitor, LY294002 was purchased from CALBIOCHEM (La Jolla, CA). Anti-mouse NKG2D monoclonal antibody CX5 (rat IgG2a isotype) was generated by immunizing rats with purified protein of mouse NKG2D kindly provided from Dr. Chris O' Callaghan (CIT). The antibody recognizes the NKG2D extracellular domain and efficiently blocks the binding of NKG2D to its ligands. Anti-mouse RAE-1 monoclonal antibody CX1 (rat IgG2b isotype) was generated by immunizing rats with CHO cells stably transfected with mouse RAE-1 γ . CX1 mAb binds strongly to RAE-1 γ and weakly to RAE-1 α and RAE-1 β , but does not react with RAE-1 δ or RAE-1 ϵ . Binding of RAE-1 to NKG2D is blocked in the presence of CX1 mAb.

Cytokine production

NK cells (2×10^5) were placed in RPMI-1640 containing 10% FCS and IL-2 (2000 U/ml), and were cultured for 18 hrs in plates precoated with the immobilized antibodies, as described previously (Ogasawara et al., 2002). To block Fc receptor-dependent activation, NK cells were pretreated with soluble anti-CD16/32 mAb 2.4G2 (BD PharMingen, San Diego, CA) (10 μ g/ml) for 30 min. The amount of IFN- γ in the culture supernatants was determined with a mouse IFN- γ -specific ELISA kit (OptEIA mouse IFN- γ set), purchased from BD PharMingen (San Diego, CA) and used according to the manufacturer's instructions. Statistical analysis was performed by using a two-sample *t*-test.

Cell lines, plasmids, and transfectants

For sequence analysis, mouse DAP10 and NKG2D were amplified from cDNA prepared from NOD NK cells by RT-PCR using oligonucleotide primers (DAP10 sense primer ATG GAC CCC CCA GGC TAC CTC, DAP10 antisense primer TCA GCC TCT GCC AGG CAT GTT, NKG2D sense primer GAA ACA GGA TCT CCC TTC and NKG2D antisense primer CCG AGA CAA TTC TCT TG). PCR products were sequenced by using standard methods. The Ba/F3 pro-B cell line was kindly provided by Dr. T. Kitamura (Univ. Tokyo) and the RMA T leukemia cell line was kindly provided by Dr. J. Ryan (UCSF). The B16 melanoma cell line was generously provided by Dr. J. Allison (UC-Berkeley). These cells were cultured in RPMI 1640 medium containing 10% FCS, 5×10^{-5} M 2-mercaptoethanol, and 2 mM glutamine. Since Ba/F3 cells are IL-3 dependent for their proliferation, the Ba/F3 cells were transfected with a mouse IL-3-cDNA plasmid to provide for autocrine growth (kindly provided by Dr. S. Tangye (Sydney, Australia). All transfectants (Ba/F3 NKG2D + DAP10, Ba/F3 NKG2D + mutant DAP10 Y-F, Ba/F3 mock, Ba/F3 RAE-1 γ , B16 mock, B16 RAE-1 ϵ , RMA mock, and RMA RAE-1 γ) were established by retroviral transduction (Kinsella and Nolan, 1996; Onihsi et al., 1996). RMA cells were transduced

by using retroviruses generated with the pMX-puro vector (Kinsella and Nolan, 1996; Onihsi et al., 1996). Other stable transfectants were established by using retroviruses generated with the pMX-pie vector. The murine NKG2D cDNA was cloned by PCR using oligonucleotide primers (Sense 5'GAGCAAATGCCATAATTACGACC -3', Anti-sense 5'- ACCGCCCTTTTCATGCAGATG-3'), and the cDNA was ligated into the pMX-pie vector. The Y residue in the cytoplasmic domain of Flag-human DAP10 (Wu et al., 2000) was mutated to F by standard PCR mutagenesis and these cDNA were ligated into pMX-neo vectors. This construct was transfected into Phoenix-A packaging cells (generously provided by Dr. Garry Nolan, Stanford) by using Lipofectamine 2000 (Gibco BRL) (Kinsella and Nolan, 1996; Onihsi et al., 1996). Two days later, the supernatants containing viruses were collected and used to infect 5×10^4 Ba/F3, and RMA cells in the presence of polybrene (8 $\mu\text{g/ml}$).

Preparation of NK cells

NK cells were prepared as described previously (Ogasawara et al., 2002). Briefly, spleen cells were incubated with anti-CD4 mAb (clone GK1.5) and anti-CD8 mAb (clone 53-6.7), and thereafter these cells were mixed with magnetic beads coated with goat anti-mouse immunoglobulin (Ig) Ab and goat anti-rat Ig Ab (Advanced Magnetic, Inc, Cambridge, MA). CD4, CD8, and surface Ig (sIg) positive cells were removed by magnetic cell sorting. The CD4-, CD8- and Ig-depleted splenocytes were stained with a PE-conjugated pan-NK cell mAb DX5 (BD PharMingen, San Diego, CA), followed by incubation with magnetic microbeads coated with anti-PE-Ab (Miltenyi Biotec Inc., Germany). Thereafter, DX5⁺ cells were isolated by magnetic cell sorting using a MACS (Miltenyi Biotec Inc., Germany). The purity of the DX5⁺ cells was more than 95%, as determined by flow cytometric analysis. The yield of purified NK cells per spleen from the different mouse

strains was as follows: C57BL/6 (number $\times 10^{-6} = 1.36 \pm 0.13$), NK1.1NOD (number $\times 10^{-5} = 8.17 \pm 0.23$), NOD (number $\times 10^{-5} = 6.14 \pm 0.15$). The purified NK cells were cultured in RPMI-1640 supplemented with 10% FCS and 5×10^{-5} M 2-mercaptoethanol in the presence of 4000 U/ml human recombinant IL-2, for 3-5 days.

Flow cytometric analysis

Cells were incubated with biotinylated anti-NKG2D mAb, biotinylated isotype control Ig (cIg) or biotinylated anti-RAE-1 γ mAb and then PE-streptavidin and anti-NK1.1-FITC or anti-DX5-FITC (BD PharMingen, San Diego, CA). To detect NKG2D ligands, we used the extracellular domain of mouse NKG2D fused to human IgG1 Fc (mNKG2D-Ig)(Cerwenka et al., 2000). A PE-conjugated goat anti-human IgG Fc γ fragment (Jackson ImmunoResearch, West Grove, PA) was used as a second step reagent. The cells (1×10^6) were stained with 0.5 μ g of mNKG2D-Ig and with 0.25 μ g of other mAbs. The incubation was carried out for 20 min, after which the cells were washed with PBS containing 0.01% NaN₃. Cells were analyzed by using a FACSCalibur (Becton Dickinson, San Jose, CA) or a small desktop Guava® Personal Cytometer with Guava ViaCount™ and Guava Express™ software (Burlingame, CA). Viable lymphocyte populations were gated based on forward and side scatters and by propidium iodide staining.

Cytotoxic Assay

Target cells were labeled with 50 μ Ci of Na₂(⁵¹Cr) O₄ for 60 min at 37°C in RPMI-1640 medium containing 10 % FCS, washed three times with medium, and used in cytotoxicity assays. ⁵¹Cr-labeled target cells (5×10^3) and effector cells were mixed in U-bottomed wells of a 96-well microtiter plate at the indicated E/T ratios in triplicate. After a 4-hr incubation, the cell-free supernatants were collected and the radioactivity was measured in

a Micro-beta counter (Wallac, Turku, Finland). The spontaneous release was less than 15% of the maximum release. The percentage of specific ⁵¹Cr release was calculated according to the following formula:

%Specific lysis = (experimental – spontaneous) release x 100 / (maximal – spontaneous) release.

A lytic unit (LU₄₀) was defined as the number of effector cells required to achieve 40% specific release. It was deduced from the mathematical slope of the line generated by plotting percent lysis vs. effector to target cell ratio. Lytic units per 10⁶ NK cells were determined by dividing lytic units per 10⁶ cells.

Quantitative PCR

Quantitative (real-time) PCR was carried out using the ABI 7700 (Applied Biosystems) according to the manufacturer's instructions. Probes for real-time PCR were purchased from Applied Biosystems. Probes were conjugated to fluorochromes (FAM) or VIC™ as specified at the 5' end, and the quencher TAMRA (6-carboxytetramethylrhodamine) or non-fluorescent quencher of MGB (minor groove binder) at the 3' end. The specific probes used were: VIC-CTT GCC ATT TTC AAA GAG ACG TTT CAG CC-TAMRA (NKG2D), FAM-CCG TGT GGG CGC ATA CAT ACA AAC A-TAMRA (DAP10), FAM-TGC AGA CAG GAA GTT -MGB (RAE-1α), FAM-ACT GAA GTG AAG AAA T-MGB (RAE-1β), FAM-CAA CCT GTG AAC GAT-MGB (RAE-1γ), FAM-CCA GCA GAT GAA G-MGB (RAE-1δ), VIC-GCC ACT GGC AAA T-MGB (RAE-1ε), VIC-TTG CCT GAT TCT GAG CCT TTT CAT TCT GCT-TAMRA (H60) and FAM-CAA ACT TTG CTT TCC CTG GTT AAG CAG TAC AGC-TAMRA (HPRT). PCR primers were as follows: RAE-1α; sense GTGAAACGATTGAAATTCTTGATACC, antisense GCTTTT CCTTGGGCTGCTTT, RAE-1β; sense AAGTAACATAAACAAGACCATGACTTCAG,

antisense TCCTCAACTTCTGGCACAAATTT, RAE-1 γ ; sense
GACGGCAAATGCCACT GAA, antisense CCACTTTGGTGTAGACACCTTGTC,
RAE-1 δ ; sense CAACTTGAC CATCAAGGCTCCTA, antisense
GATAAGTATTTACCCACGAAGCA, RAE-1 ϵ ; sense
CAGGTGACCCAGGGAAGATG, antisense CTCAACTCCTGGCACAAATCG, DAP10;
sense GCGGTCATGTCACTCCTAATTG, antisense ACCATCTTCTTGGG CAGGC,
NKG2D; sense CGATTCACCTTAACACATTGATG, antisense GGGACTT
CCTTGTTGCACAATAC, HPRT; sense TGG AAA GAA TGT CTT GAT TGT TGA A,
antisense AGC TTG CAA CCT TAA CCA TTT TG, H60; sense GAG CCA CCA GCA
AGA GCA A, antisense CCA GTA TGG TCC CCA GAT AGC T. Total RNA was treated
with DNase I, and then first-strand cDNA was synthesized by using random hexamer
primers. The cycling conditions for real-time PCR were: 50°C for 10 min, followed by 45
cycles of 95°C for 30 sec, and 60°C for 2 min. Data were analyzed by using the Sequence
Detector v1.7 Analysis Software (Applied Biosystems).

Acknowledgements

We thank Marina Abramova, Gregory L. Szot, and Paul Wegfahrt for expert assistance with the NOD mice experiments. This work is supported by a UCSF Diabetes Center Pilot & Feasibility Grant, NIH grant CA89189 and JDRFI 4-1999-841. K. O. is supported by Human Frontier Science Program Long-term Fellowship. J. A. H. is supported by an Irvington Foundation Fellowship. L.L.L. is an American Cancer Society Research Professor.

References

- Abrams, S. I., and Brahmi, Z. (1988). Target cell directed NK inactivation. Concomitant loss of NK and antibody-dependent cellular cytotoxicity activities, *J Immunol* *140*, 2090-5.
- Attallah, A. M., Abdelghaffar, H., Fawzy, A., Alghraoui, F., Alijani, M. R., Mahmoud, L. A., Ghoneim, M. A., and Helfrich, G. B. (1987). Cell-mediated immunity and biological response modifiers in insulin- dependent diabetes mellitus complicated by end-stage renal disease, *Int Arch Allergy Appl Immunol* *83*, 278-83.
- Bach, J. F. (1994). Insulin-dependent diabetes mellitus as an autoimmune disease, *Endocr Rev* *15*, 516-42.
- Bauer, S., Groh, V., Wu, J., Steinle, A., Phillips, J. H., Lanier, L. L., and Spies, T. (1999). Activation of natural killer cells and T cells by NKG2D, a receptor for stress-inducible MICA, *Science* *285*, 727-730.
- Biron, C. A., Nguyen, K. B., Pien, G. C., Cousens, L. P., and Salazar-Mather, T. P. (1999). Natural killer cells in antiviral defense: function and regulation by innate cytokines, *Annu Rev Immunol* *17*, 189-220.
- Brodsky, F. M., Chen, C. Y., Knuehl, C., Towler, M. C., and Wakeham, D. E. (2001). Biological basket weaving: formation and function of clathrin-coated vesicles, *Annu Rev Cell Dev Biol* *17*, 517-68.
- Cameron, M. J., Meagher, C., and Delovitch, T. L. (1998). Failure in immune regulation begets IDDM in NOD mice, *Diabetes Metab Rev* *14*, 177-85.
- Carnaud, C., Gombert, J., Donnars, O., Garchon, H., and Herbelin, A. (2001). Protection against diabetes and improved NK/NKT cell performance in NOD.NK1.1 mice congenic at the NK complex, *J Immunol* *166*, 2404-11.
- Castano, L., and Eisenbarth, G. S. (1990). Type-I diabetes: a chronic autoimmune disease of human, mouse, and rat, *Annu Rev Immunol* *8*, 647-79.

Cefai, D., Schneider, H., Matangkasombut, O., Kang, H., Brody, J., and Rudd, C. E. (1998). CD28 receptor endocytosis is targeted by mutations that disrupt phosphatidylinositol 3-kinase binding and costimulation, *J Immunol* *160*, 2223-30.

Cerwenka, A., Bakker, A. B., McClanahan, T., Wagner, J., Wu, J., Phillips, J. H., and Lanier, L. L. (2000). Retinoic acid early inducible genes define a ligand family for the activating NKG2D receptor in mice, *Immunity* *12*, 721-7.

Cerwenka, A., and Lanier, L. L. (2001). Natural killer cells, viruses and cancer, *Nat Rev Immunol* *1*, 41-9.

Chang, C., Dietrich, J., Harpur, A. G., Lindquist, J. A., Haude, A., Loke, Y. W., King, A., Colonna, M., Trowsdale, J., and Wilson, M. J. (1999). Cutting edge: KAP10, a novel transmembrane adapter protein genetically linked to DAP12 but with unique signaling properties, *J Immunol* *163*, 4651-4.

Ghosh, S., Palmer, S. M., Rodrigues, N. R., Cordell, H. J., Hearne, C. M., Cornall, R. J., Prins, J. B., McShane, P., Lathrop, G. M., Peterson, L. B., and et al. (1993). Polygenic control of autoimmune diabetes in nonobese diabetic mice, *Nat Genet* *4*, 404-9.

Groh, V., Wu, J., Yee, C., and Spies, T. (2002). Tumour-derived soluble MIC ligands impair expression of NKG2D and T-cell activation, Nature *419*, 734-8.

Ho, E. L., Heusel, J. W., Brown, M. G., Matsumoto, K., Scalzo, A. A., and Yokoyama, W. M. (1998). Murine Nkg2d and Cd94 are clustered within the natural killer complex and are expressed independently in natural killer cells, *Proc Natl Acad Sci U S A* *95*, 6320-5.

Jamieson, A. M., Diefenbach, A., McMahon, C. W., Xiong, N., Carlyle, J. R., and Raulet, D. H. (2002). The role of the NKG2D immunoreceptor in immune cell activation and natural killing, *Immunity* *17*, 19-29.

Jewett, A., and Bonavida, B. (1995). Target-induced anergy of natural killer cytotoxic function is restricted to the NK-target conjugate subset, *Cell Immunol* *160*, 91-7.

12/12/02 1:33 PM

Deleted: .

Kataoka, S., Satoh, J., Fujiya, H., Toyota, T., Suzuki, R., Itoh, K., and Kumagai, K. (1983). Immunologic aspects of the nonobese diabetic (NOD) mouse. Abnormalities of cellular immunity, *Diabetes* 32, 247-53.

Kinsella, T. M., and Nolan, G. P. (1996). Episomal vectors rapidly and stably produce high-titer recombinant retrovirus, *Human Gene Therapy* 7, 1405-1413.

Lanier, L. L. (1998). NK cell receptors, *Annu Rev Immunol* 16, 359-393.

Mizuki, N., Ota, M., Kimura, M., Ohno, S., Ando, H., Katsuyama, Y., Yamazaki, M., Watanabe, K., Goto, K., Nakamura, S., *et al.* (1997). Triplet repeat polymorphism in the transmembrane region of the MICA gene: a strong association of six GCT repetitions with Behcet disease, *Proc Natl Acad Sci U S A* 94, 1298-303.

Nair, M. P., Lewis, E. W., and Schwartz, S. A. (1986). Immunoregulatory dysfunctions in type I diabetes: natural and antibody- dependent cellular cytotoxic activities, *J Clin Immunol* 6, 363-72.

Negishi, K., Waldeck, N., Chandy, G., Buckingham, B., Kershner, A., Fisher, L., Gupta, S., and Charles, M. A. (1986). Natural killer cell and islet killer cell activities in type 1 (insulin- dependent) diabetes, *Diabetologia* 29, 352-7.

Norris, S., Kondeatis, E., Collins, R., Satsangi, J., Clare, M., Chapman, R., Stephens, H., Harrison, P., Vaughan, R., and Donaldson, P. (2001). Mapping MHC-encoded susceptibility and resistance in primary sclerosing cholangitis: the role of MICA polymorphism, *Gastroenterology* 120, 1475-82.

Ogasawara, K., Yoshinaga, S. K., and Lanier, L. L. (2002). Inducible Costimulator Costimulates Cytotoxic Activity and IFN-gamma Production in Activated Murine NK Cells, *J Immunol* 169, 3676-85.

Onihsi, M., Kinoshita, S., Morikawa, Y., Shibuya, A., Phillips, J., Lanier, L. L., Gorman, D. M., Nolan, G. P., Miyajima, A., and Kitamura, T. (1996). Applications of retrovirus-

mediated expression cloning, *Exp Hematology* 24, 324-329.

Perussia, B., and Trinchieri, G. (1981). Inactivation of natural killer cell cytotoxic activity after interaction with target cells, *J Immunol* 126, 754-8.

Poulton, L. D., Smyth, M. J., Hawke, C. G., Silveira, P., Shepherd, D., Naidenko, O. V., Godfrey, D. I., and Baxter, A. G. (2001). Cytometric and functional analyses of NK and NKT cell deficiencies in NOD mice, *Int Immunol* 13, 887-96.

Rapoport, I., Miyazaki, M., Boll, W., Duckworth, B., Cantley, L. C., Shoelson, S., and Kirchhausen, T. (1997). Regulatory interactions in the recognition of endocytic sorting signals by AP-2 complexes, *EMBO J* 16, 2240-50.

Rogner, U. C., Boitard, C., Morin, J., Melanitou, E., and Avner, P. (2001). Three loci on mouse chromosome 6 influence onset and final incidence of type I diabetes in NOD.C3H congenic strains, *Genomics* 74, 163-71.

Schneider, H., Martin, M., Agarraberes, F. A., Yin, L., Rapoport, I., Kirchhausen, T., and Rudd, C. E. (1999). Cytolytic T lymphocyte-associated antigen-4 and the TCR zeta/CD3 complex, but not CD28, interact with clathrin adaptor complexes AP-1 and AP-2, *J Immunol* 163, 1868-79.

Shultz, L. D., Schweitzer, P. A., Christianson, S. W., Gott, B., Schweitzer, I. B., Tennent, B., McKenna, S., Mobraaten, L., Rajan, T. V., Greiner, D. L., and et al. (1995). Multiple defects in innate and adaptive immunologic function in NOD/LtSz-scid mice, *J Immunol* 154, 180-91.

Sorkin, A., and Carpenter, G. (1993). Interaction of activated EGF receptors with coated pit adaptins, *Science* 261, 612-5.

Sugimura, K., Ota, M., Matsuzawa, J., Katsuyama, Y., Ishizuka, K., Mochizuki, T., Mizuki, N., Seki, S. S., Honma, T., Inoko, H., and Asakura, H. (2001). A close relationship of triplet repeat polymorphism in MHC class I chain-related gene A (MICA) to the disease

susceptibility and behavior in ulcerative colitis, *Tissue Antigens* 57, 9-14.

Timonen, T., Saksela, E., Ranki, A., and Hayry, P. (1979). Fractionation, morphological and functional characterization of effector cells responsible for human natural killer activity against cell-line targets, *Cell Immunol* 48, 133-48.

Touitou, I., Picot, M. C., Domingo, C., Notarnicola, C., Cattan, D., Demaille, J., and Kone-Paut, I. (2001). The MICA region determines the first modifier locus in familial Mediterranean fever, *Arthritis Rheum* 44, 163-9.

Trinchieri, G. (1989). Biology of natural killer cells, *Adv Immunol* 47, 187-376.

Wallace, G. R., Verity, D. H., Delamaine, L. J., Ohno, S., Inoko, H., Ota, M., Mizuki, N., Yabuki, K., Kondiatis, E., Stephens, H. A., *et al.* (1999). MIC-A allele profiles and HLA class I associations in Behcet's disease, *Immunogenetics* 49, 613-7.

Wicker, L. S., Todd, J. A., and Peterson, L. B. (1995). Genetic control of autoimmune diabetes in the NOD mouse, *Annu Rev Immunol* 13, 179-200.

Wu, J., Cherwinski, H., Spies, T., Phillips, J. H., and Lanier, L. L. (2000). DAP10 and DAP12 form distinct, but functionally cooperative, receptor complexes in natural killer cells, *J Exp Med* 192, 1059-68.

Wu, J., Song, Y., Bakker, A. B. H., Bauer, S., Groh, V., Spies, T., Lanier, L. L., and Phillips, J. H. (1999). An activating receptor complex on natural killer and T cells formed by NKG2D and DAP10, *Science* 285, 730-732.

Yokoyama, W. M., and Seaman, W. E. (1993). The Ly-49 and NKR-P1 gene families encoding lectin-like receptors on natural killer cells: The NK gene complex, *Ann Rev Immunol* 11, 613-635.

Figure legends

Figure 1. NKG2D-dependent cytotoxicity and IFN- γ production by NK1.1 NOD and NOD NK cells. **a.** The cytotoxicity of C57BL/6, NK1.1 NOD and NOD NK cells against YAC-1 target cells was blocked by anti-mouse NKG2D mAb. Purified and IL-2 activated C57BL/6, NK1.1 NOD and NOD NK cells were pre-cultured with an anti-NKG2D mAb (rat IgG2a isotype) or an isotype-control rat Ig for 30 min and then mixed with target cells. The anti-NKG2D mAb (squares) or the cIg (circles) was present throughout the cytotoxic assay. Cytotoxicity was measured by ^{51}Cr release after 4 hr. Lytic unit (LU_{40}) against YAC-1 targets were as follows: C57BL/6 ($\text{LU}_{40}=1.17\times 10^6$), NK1.1NOD ($\text{LU}_{40}=7.61\times 10^4$) and NOD ($\text{LU}_{40}=6.47\times 10^4$). **b.** NKG2D-dependent cytotoxicity mediated by NK1.1 NOD and NOD NK cells. NK cells were purified and activated with IL-2 as in Fig. 1a. Cytotoxic activity against RAE-1 γ transfected Ba/F3 cells and mock Ba/F3 transfectants was tested by using a 4-h ^{51}Cr release assay. Data are represented as the mean % cytotoxicity \pm SD (triplicates). Similar results were obtained in two independent experiments. **c.** NKG2D-dependent IFN- γ production by NK1.1 NOD and NOD NK cells. NK cells were stimulated with immobilized mAb ($1\ \mu\text{g ml}^{-1}$) or IL-12 $1\ \text{ng ml}^{-1}$ for 18 hr. Conditions were as follows: anti-NKG2D mAb (filled column), rat cIg (open column), anti-NK1.1 mAb (hatched column) and IL-12 (gray column). Culture supernatants were collected for the measurement of IFN- γ by ELISA. Differences in IFN- γ production of NK cells from C57BL/6, NOD and NK1.1 NOD induced by anti-NKG2D mAb stimulation were highly significant, * $P<0.01$; C57BL/6 versus NK1.1 NOD, $P<0.01$; C57BL/6 versus NOD.

Figure 2. NKG2D expression on NOD NK cells. **a.** NKG2D expression was modulated on NK1.1NOD and NOD NK cells. Purified NK cells prepared from C57BL/6,

NK1.1NOD and NOD mice were cultured with IL-2 for 4 days. These NK cells were stained with biotinylated anti-NKG2D mAb, biotinylated isotype control Ig (cIg), PE-conjugated anti-CD44 mAb, and PE-conjugated anti-NK1.1 mAb. To detect NKG2D expression, PE-conjugated streptavidin was used as the second step reagent. In upper panel, the dotted line shows isotype cIg staining and the thick line shows NKG2D expression on NK cells. Similar results were observed when an H-60 Ig Fc fusion protein was used to detect NKG2D (data not shown). The dotted lines show isotype cIg staining (middle and lower panel). The thick line represents CD44 (middle panel) or NK1.1 (lower panel) expression on these NK cells. **b.** NKG2D and DAP10 transcripts in C57BL/6, NK1.1 NOD and NOD NK cells quantitated by real-time PCR. Total RNA was prepared from purified and IL-2 activated NK cells from C57BL/6, NK1.1NOD and NOD mice. Real-time PCR was performed as described in the Methods section. Data were normalized by the amount of HPRT mRNA. Data are shown as the mean cycles of normalized NKG2D or DAP10 expression \pm SD (triplicates). **c.** NKG2D ligands were expressed on NK1.1 NOD and NOD NK cells. NK cells were prepared as in Fig. 2a. NK cells were stained with a mouse NKG2D-human Ig Fc fusion protein (NKG2D Ig) or control human Ig (cIg). To detect the binding of NKG2D-Ig, a PE-conjugated anti-human IgG antibody (anti-human Ig PE) was used as a second step antibody. The dotted line represents control human Ig staining on NK cells. The thick line shows NKG2D ligand expression on NK cells. **d.** NKG2D ligand transcripts in C57BL/6, NK1.1 NOD and NOD NK cells. Real-time PCR was performed as in Fig. 2b. Data were normalized to the amount of HPRT mRNA. N. D. is not detected. **e.** Expression of RAE-1 on NK1.1 NOD and NOD NK cells. NK cells were prepared as in Fig. 2a. NK cells were stained with biotinylated anti-RAE-1 mAb (CX1) or biotinylated isotype cIg and then stained with PE-conjugated streptavidin. The dotted line shows isotype cIg staining and the thick line shows RAE-1

expression on NK cells. These results were reproducible (3 independent experiments) and representative data are shown. Anti-RAE-1 mAb CX1 predominantly reacts with RAE-1 γ , but also reacts weakly with RAE-1 α and RAE-1 β , but not H-60.

Figure 3. Ligand-induced NKG2D modulation. **a.** Modulation of NKG2D on NK cells by co-culture with ligand-bearing cells. NK cells were prepared from C57BL/6 mice and co-cultured with mock-transfected B16 melanoma cells or RAE-1 ϵ transfected B16 cells in the presence of IL-2 (500U/ml). After 48-hrs culture, NK cells were co-stained with anti-NK1.1 mAb and anti-NKG2D mAb. The dotted line shows cIg staining and the thick line shows NKG2D expression on NK1.1⁺NK cells (upper panel). Lower panel shows CD44 expression on these NK cells (thick line). **b.** Cytotoxicity against YAC-1 was decreased in NK cells co-cultured with RAE-1⁺B16 transfectants. NK cells were co-cultured with RAE-1⁺B16 or mock B16 transfectants as in Fig. 3a. **c.** NKG2D-dependent cytotoxicity was decreased in NK cells co-cultured with RAE-1⁺B16 transfectants. NK cells were co-cultured with RAE-1⁺B16 (filled circles) and mock B16 transfectants (open circles) as in Fig. 3a. Cytotoxic activity against RAE-1 γ bearing Ba/F3 cells (Ba/F3 RAE-1 γ) or mock transfectants (Ba/F3 mock) was tested by using a 4-h ⁵¹Cr release assay. Data are represented as the mean % cytotoxicity \pm SD (triplicates). Similar results were obtained in two independent experiments. **d.** IFN- γ production induced by cross-linking with anti-NKG2D mAb was reduced in NK cells previously co-cultured with RAE-1⁺B16 transfectants. NK cells co-cultured with mock or RAE-1 B16 transfectants were harvested, purified from the residual tumor cells and then were stimulated with immobilized mAb (3 μ g ml⁻¹) for 18 hr. Culture supernatants were collected for measurement of IFN- γ by ELISA. The amount of IFN- γ produced by NK cells cultured with the plated coated with control rat IgG (open column), anti-NKG2D mAb (filled column), or anti-NK1.1 mAb

(hatched column). As a positive control for cytokine production, NK cells were cultured with IL-12 (gray column). Data are represented as the mean $\text{ng ml}^{-1} \pm \text{SD}$ (triplicates). Differences in IFN- γ production of NK cells co-cultured with B16 or RAE-1 ϵ □□ induced by anti-NKG2D mAb stimulation were highly significant, * $P < 0.01$; NK+B16 mock versus NK+B16 RAE-1 ϵ . e. NKG2D was modulated *in vivo* on NK cells in mice bearing a RAE-1 $^+$ tumor. RAE-1 $^+$ RMA (1×10^7) or mock-transfected RMA cells (1×10^7) were injected directly into the spleen of C57BL/6 mice. After 5 days, splenic NK cells were harvested and expression of NKG2D expression was analyzed. f. Recovery of NKG2D expression in the absence of ligand. C57BL/6 NK cells were co-cultured with irradiated RAE-1 ϵ transfected B16 or mock-transfected B16 cells. After 24 hrs, modulation of NKG2D was confirmed on cells co-cultured with ligand-bearing tumor cells. NK cells were harvested, cultured in IL-2 only for 1 day and then stained with anti-NK1.1 mAb and anti-NKG2D mAb. The dotted line shows cIg staining and the thick line shows NKG2D expression on NK1.1 $^+$ NK cells.

Figure 4. Modulation of NKG2D is regulated by the YxxM motif of DAP10. a. Ba/F3 cells transfected with NKG2D and DAP10 (Ba/F3 NKG2D-DAP10) were co-cultured with RMA mock transfectants or RMA cells transfected with RAE-1 γ . The NKG2D - DAP10 Ba/F3 transfectants also expressed GFP as a result of transduction with an IRES-GFP retroviral vector. After co-culture and prior to staining with anti-NKG2D mAb or H-60-Ig fusion protein, cells were washed briefly in an acidic buffer (RPMI 1640 adjusted to pH 4.0 with HCl with 3% FCS). This was done to elute any shed RAE-1 from the NKG2D transfectant, which may prevent detection of NKG2D because of masking by ligand. As a positive control, we demonstrated that this acid treatment successfully removed H-60-Ig Fc fusion protein from Ba/F3 NKG2D-DAP10 cells (data not shown). b. Detection of

intracellular NKG2D after modulation. Ba/F3 NKG2D-DAP10 cells were co-cultured with RMA or RMA RAE-1 γ cells for 14 hrs. After co-culture, cells were fixed in 1% paraformaldehyde and permeabilized by saponin. Then, these cells were stained with anti-NKG2D mAb. (Note that the staining intensity of anti-NKG2D mAb was less on fixed cells, compared with fresh cells, probably because fixation affected the antigen.) **c.** NKG2D modulation was not influenced by lysosome inhibitors. Ba/F3 NKG2D-DAP10 cells were co-cultured with RMA cells or RMA RAE-1 γ in the presence or absence of lysosome inhibitors, NH₄Cl (50mM) or chloroquine (100 μ M) for 6 hrs. Data using NH₄Cl (50 mM) are shown. Similar results were obtained in using the lysosome inhibitor, chloroquine (100 μ M). **d.** Clathrin-dependent endocytosis is involved in NKG2D down modulation. Ba/F3 NKG2D-DAP10 cells were co-cultured with RMA or RMA RAE-1 γ cells in the presence or absence of medium containing 0.45 M sucrose. The percentage reduction of NKG2D surface expression in the presence of ligand was calculated as follows: % of NKG2D surface expression = mean fluorescence of Ba/F3 NKG2D-DAP10 cells co-cultured with RMA RAE-1 γ x 100 / mean fluorescence of Ba/F3 NKG2D-DAP10 cells co-cultured with RMA. **e.** PI3 kinase was involved in NKG2D modulation. Ba/F3 NKG2D-DAP10 cells were co-cultured with RMA or RMA RAE-1 γ cells for 14 hrs in the presence of PI3 kinase inhibitor, LY294002 (30 μ M). The dotted line shows cIg staining. The gray histogram shows NKG2D expression on Ba/F3 NKG2D-DAP10 cells co-cultured with RMA RAE-1 γ cells in the presence of DMSO (mean=15.1) or LY294002 (mean =38.2) and thick line shows NKG2D expression on Ba/F3 NKG2D-DAP10 cells co-cultured with RMA mock transfectants in the presence of DMSO (mean = 63.9) or LY294002 (mean = 66.2). **f.** The YxxM motif of DAP10 regulates NKG2D modulation. Ba/F3 NKG2D-DAP10 cells or Ba/F3 NKG2D-mutant DAP10 Y-F cells were co-cultured with RMA or RMA RAE-1 γ cells for 14 hrs. The dotted line shows cIg staining. The gray

histogram shows NKG2D expression on Ba/F3 NKG2D-DAP10 cells (upper panel) or Ba/F3 NKG2D-DAP10 (Y-F) mutants (lower panel) co-cultured with RMA RAE-1 γ . The thick lines show NKG2D expression on Ba/F3 NKG2D-DAP10 cells (upper panel) or Ba/F3 NKG2D-DAP10 (Y-F) mutants (lower panel) co-cultured with RMA. Mean fluorescence is as follows: NKG2D expression on Ba/F3 NKG2D-DAP10 cells co-cultured with RMA (mean =148.64), Ba/F3 NKG2D-DAP10 cells co-cultured with RMA RAE-1 γ (mean =35.42), NKG2D expression on Ba/F3 NKG2D-DAP10 (Y-F) cells co-cultured with RMA (mean =110.89), Ba/F3 NKG2D-DAP10 cells co-cultured with RMA RAE-1 γ (mean =71.5), These results were reproducible (2 independent experiments) and representative data are shown.

Fig. 1

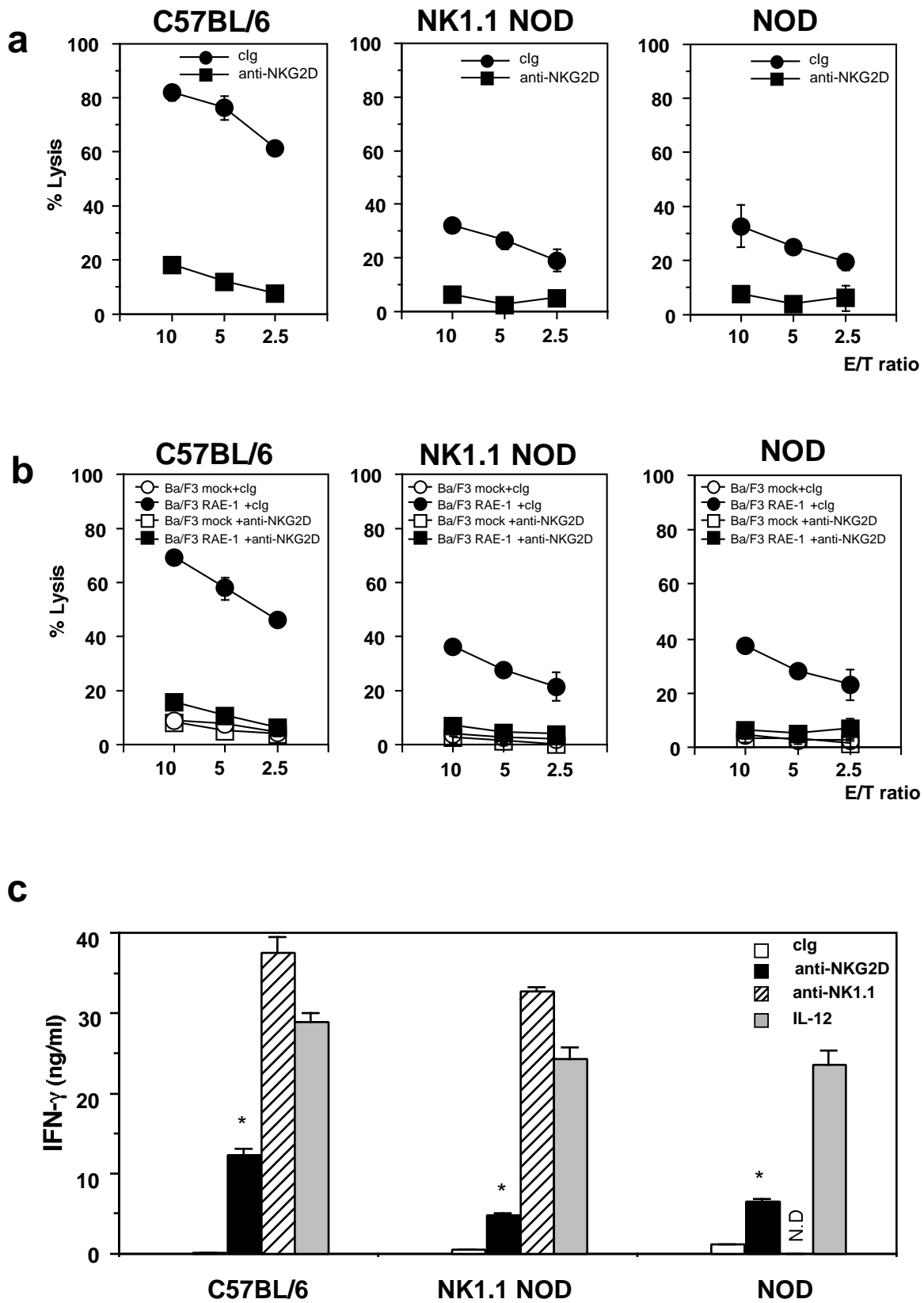


Fig. 2

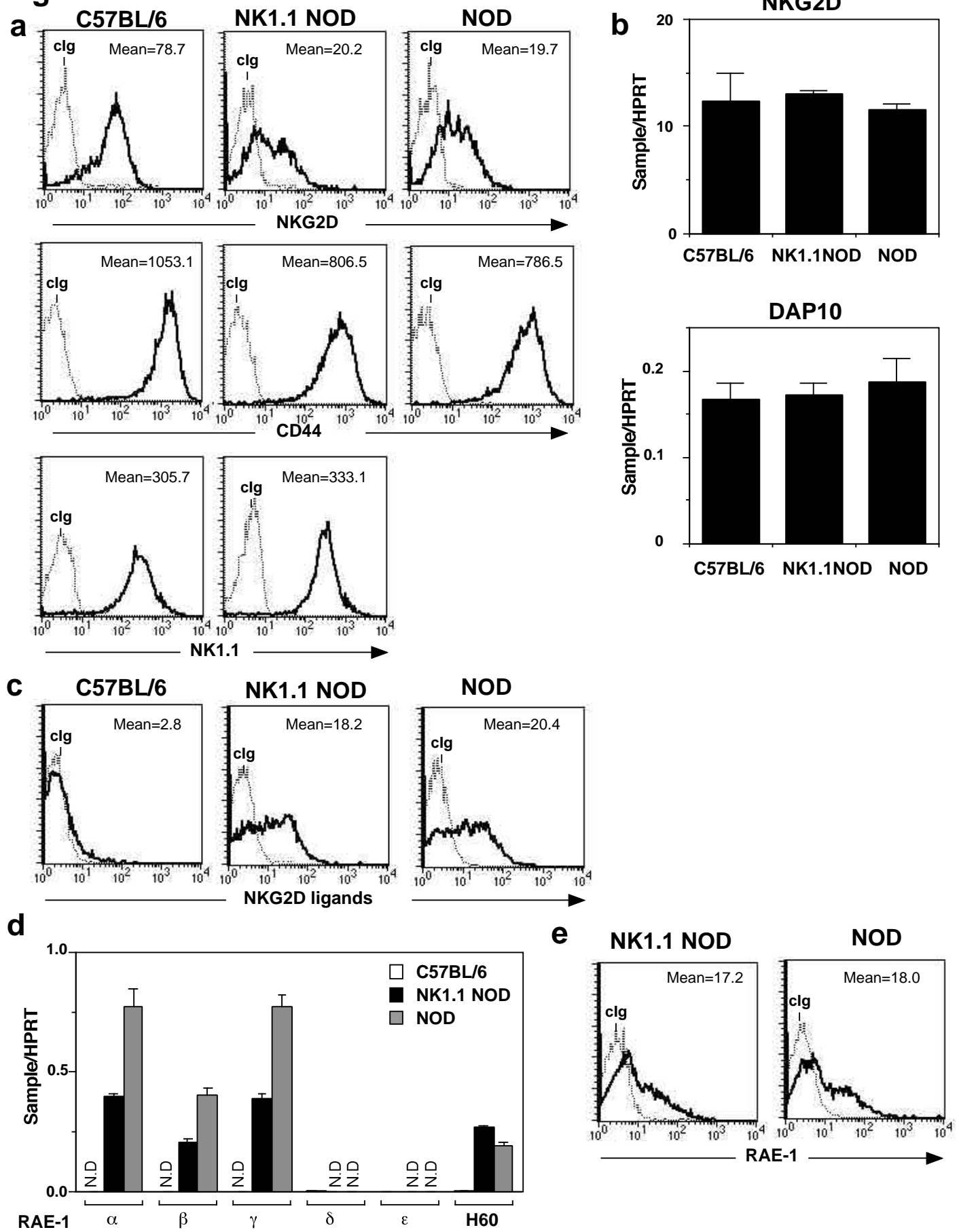


Fig. 3

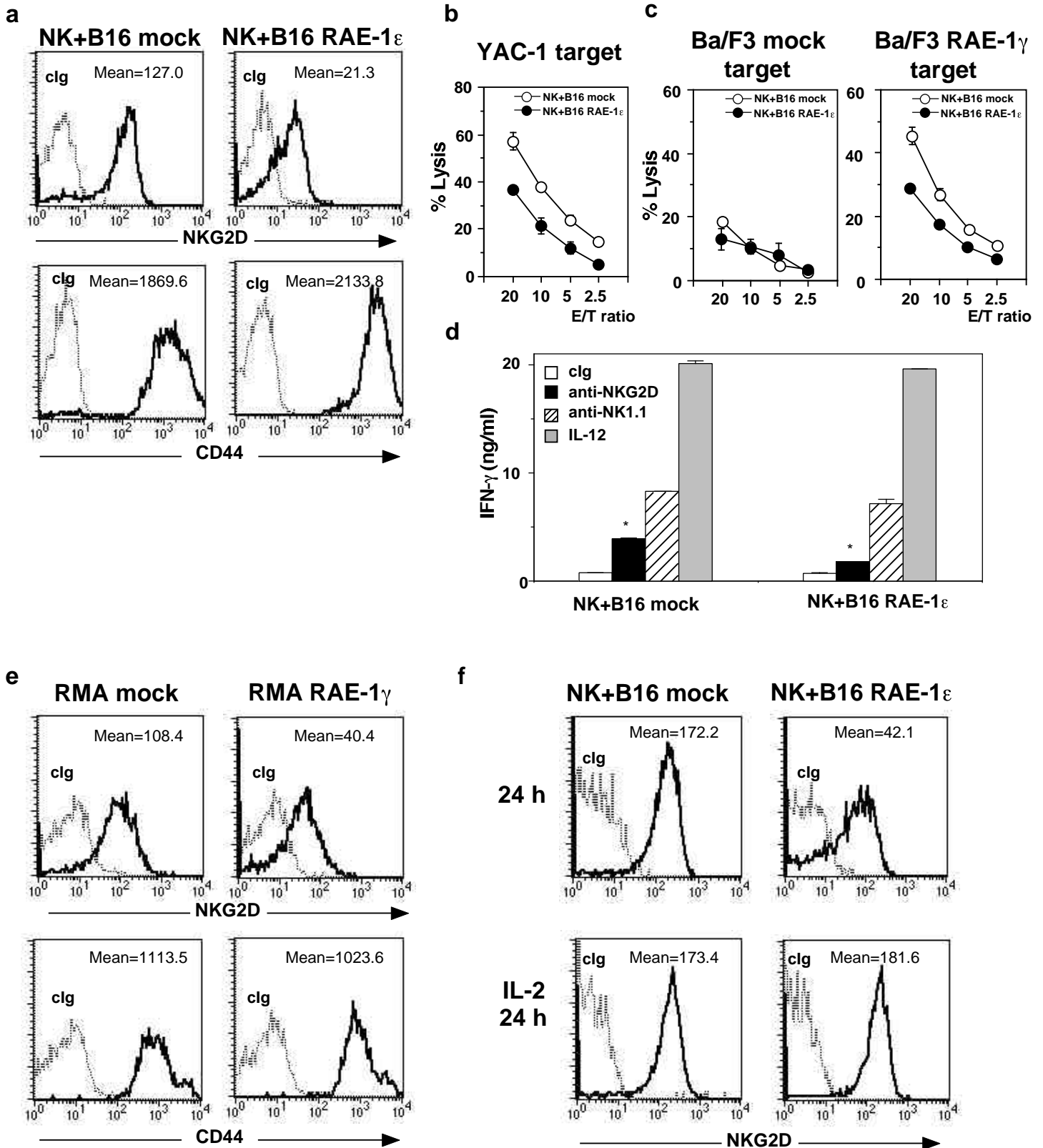


Fig. 4